Computers in Biology and Medicine 207 (2026) 111627

Contents lists available at ScienceDirect

Computers in Biology and Medicine

journal homepage: www.elsevier.com/locate/compbiomed

Does maternal respiration modulate maternal-fetal cardiovascular coupling?

G. Steyde[a,b], A. Galli[b,*], E. Peri[b], M.B. Van der Hout-van der Jagt[c,b], J.O.E.H. Van Laar[c,b], M.G. Signorini[a], M. Mischi[b]

[a] Department of Electronics, Information and Bioengineering, Politecnico di Milano, Piazza Leonardo da Vinci, 32, Milan, 20133, Lombardy, Italy
[b] Department of Electrical Engineering, Eindhoven University of Technology, De Groene Loper 19, Eindhoven, 5612AP, Noord-Brabant, the Netherlands
[c] Department of Gynaecology and Obstetrics, Máxima Medical Center, Dominee Theodor Fliednerstraat 1, Veldhoven, 5631BM, Noord-Brabant, the Netherlands

HIGHLIGHTS

- Maternal–fetal cardiac coupling was assessed in over 300 healthy and pathological pregnancies.
- Maternal respiration modulates both maternal and fetal heart rate dynamics.
- Conotruncal anomalies are linked to a weakened respiratory-driven influence on fetal heart rate.
- Accounting for respiration in MFCC analysis enables more accurate pregnancy monitoring strategies.

ARTICLE INFO

Keywords:
Coupling analysis
Fetal heart rate
Partial directed coherence
Pregnancy monitoring
Respiration

ABSTRACT

Objective: Maternal Fetal Cardiac Coupling (MFCC) is an understudied physiological phenomenon that could play a key role in the understanding and early detection of pregnancy-related pathologies. In this study, we aimed to investigate the role of maternal respiration in the short-term directed interactions between the maternal heart rate (MHR) and fetal heart rate (FHR) in healthy fetuses. Additionally, we investigated how such coupling patterns might be impaired in fetuses affected by conotruncal anomalies (CTA). *Methods*: FHR, MHR and maternal respiration were extracted from non-invasive abdominal electrophysiological recordings from over 300 pregnant women in the second trimester of gestation. Linear coupling metrics—Directed Coherence (DC), Partial Directed Coherence (PDC), and generalized PDC (gPDC)—were computed with and without including the respiratory signal in the Multivariate Autoregressive model. Results between healthy and CTA fetuses were compared. *Results*: Maternal respiration Granger-causes both the FHR and the MHR, suggesting respiration is a dominant source of directional influence in MFCC during the second trimester. Preliminary results suggest that the directed interaction from maternal respiration to the FHR is reduced in fetuses with CTA. *Conclusion*: Maternal respiration plays a main role in the physiological phenomenon of MFCC. *Significance*: This work sheds light on a fundamental dynamic regulating MFCC, which might improve the monitoring of pregnancy-related cardiovascular pathologies and pave the way for their early diagnosis.

1. Introduction

Several major pregnancy-related pathologies such as preeclampsia, fetal growth restriction, and fetal asphyxia originate from maladaptive responses of the maternal cardiovascular system (mCVS) and the uterine vasculature during gestation [1], or are linked to impairments in the development of the fetal cardiovascular system (fCVS) and the placenta [2].

The mCVS and the fCVS are deeply interconnected. Indeed, fCVS and mCVS dysfunctions are often present simultaneously [1,3], which suggests that pathologies might arise from the impaired bidirectional interaction between the fetus and mother. The (patho)physiological interaction among these components could be a crucial factor in unraveling the mechanisms responsible for pregnancy pathologies and could offer the possibility of identifying pathological conditions before symptoms emerge.

Multiple studies have investigated the relations between the mCVS and fCVS, both over multiple hours (long-term) [4] and within a few minutes (short-term) [5]. Specifically, most research on maternal-fetal

* Corresponding author.
Email address: a.galli@tue.nl (A. Galli).

https://doi.org/10.1016/j.compbiomed.2026.111627
Received 2 July 2025; Received in revised form 15 December 2025; Accepted 11 March 2026
Available online 18 March 2026

cardiac coupling (MFCC) focuses on modeling the relation between the maternal heart rate (MHR) and the fetal heart rate (FHR) [5–10] because they are representative of the overall functioning of the mCVS and fCVS, respectively. For instance, Khandoker and colleagues found a Granger causal influence of the FHR on the MHR during the second trimester, which decreased during the third, accompanied by a significant increase in the coupling strength from the MHR to the FHR [6]. Such findings were reported by the same group using both the linear Partial Directed Coherence (PDC) [6] and the non-linear Transfer Entropy [8] to quantify Granger causality. The association between MHR and FHR patterns was also investigated using high-resolution joint symbolic dynamics in [7]. The authors found a stronger association between maternal slow heart rate variations and FHR decreases in various fetal cardiac abnormalities (e.g., congenital heart defects, tachycardia, and atrioventricular block) compared to normal cases. In [11], cross-spectral analysis applied to ECG-derived FHR and MHR series in near-term fetuses revealed a significant correlation, particularly around 0.4 Hz. This frequency band is associated with breathing in adults, which is reflected in the MHR through the well-known phenomenon of Respiratory Sinus Arrhythmia (RSA) [12]. This suggests a potential influence of maternal breathing on MFCC. A similar relationship was confirmed in a lamb model, where a clear correlation between maternal respiration and the FHR was reported [13]. Moreover, more recent research in humans showed that changes in maternal breathing patterns can significantly affect the FHR. For instance, Leeuwen et al. [14] found that paced maternal breathing could modulate MHR through RSA, which in turn influences the FHR, suggesting a direct synchronization mechanism between the maternal and fetal systems.

To summarize, existing literature indicates that MFCC is present and varies with gestational age and maternal–fetal health. Its underlying causes, however, remain unclear and may involve secondary processes [10]. Evidence points to maternal respiration as a contributing factor, but it is uncertain whether this interaction occurs indirectly via maternal heart rate—modulated by respiration through RSA—or through a more direct effect on the fetal heart rate.

To address this open question, this study takes a novel approach by directly considering the maternal respiratory signal, offering new insights into the dynamics underlying MFCC. Indeed, we propose to explicitly include the respiratory signal in the analysis, in order to assess whether:

1. maternal respiration influences MFCC indirectly through RSA, or
2. maternal respiration has a direct coupling with the FHR.

To answer the research question, we adopted well-established methods for assessing cardiovascular signal interactions based on Granger causality in the frequency domain. These approaches have been extensively validated in cardiovascular and respiratory physiology, widely applied in previous studies [7,15–18] and shown to yield physiologically meaningful results [19]. Their robust validation, interpretability, and clinical relevance make them the most appropriate choice for our investigation and ensure comparability with existing literature in cardiovascular signal interaction. In particular, we analyzed short-term Granger-causal interactions of MHR, FHR, and respiration using PDC, Directed Coherence (DC), and generalized PDC (gPDC). Analyses were conducted using trivariate autoregressive (AR) models, which account for all interactions simultaneously, and pairwise bivariate AR models to facilitate comparison with previous studies and better understand the nature of the relationships.

Analyses were conducted in a large cohort of healthy fetuses in the second trimester of gestation. The results obtained suggest that at the considered gestational age, maternal respiration acts as the primary source of predictive information underlying the relationship between MHR and FHR. No significant direct information flow between the FHR and the MHR was identified when respiration was included in the model.

The same analysis was also conducted in a small sample of fetuses affected by conotruncal anomalies (CTA). CTA is a group of congenital heart defects affecting the cardiac outflow tract, which accounts for approximately 25% of all cases of congenital heart defects [20]. With current technologies, accurate antenatal diagnosis of CTA remains challenging, and the pathology is often identified only postnatally [21,22]. Our findings suggest that MFCC may be altered in fetuses with CTA, supporting the hypothesis that the analytical approach proposed in this study could pave the way for earlier detection, ultimately contributing to improved pregnancy outcomes [23].

The paper is organized in the following way: in Section 2 we describe the sample population and experimental setup, the methodologies employed to estimate the signals of interest (FHR, MHR and respiration), and the coupling measures analyzed; in Section 3 we report the values of the coupling metrics and their significance in healthy fetuses and compare them with values obtained in CTA-affected fetuses. In Section 4, we interpret the results obtained and outline their possible impact and future developments. Finally, Section 5 reports a few conclusive remarks.

2. Methods

A high-level overview of the methodology is shown in Fig. 1 and described in the following sections. Abdominal ECG recordings (Section 2.1) were used to extract the time series of interest (FHR, MHR, and respiration), which were segmented into 2-minute windows (Section 2.2). For each window, a linear model was fitted and coupling

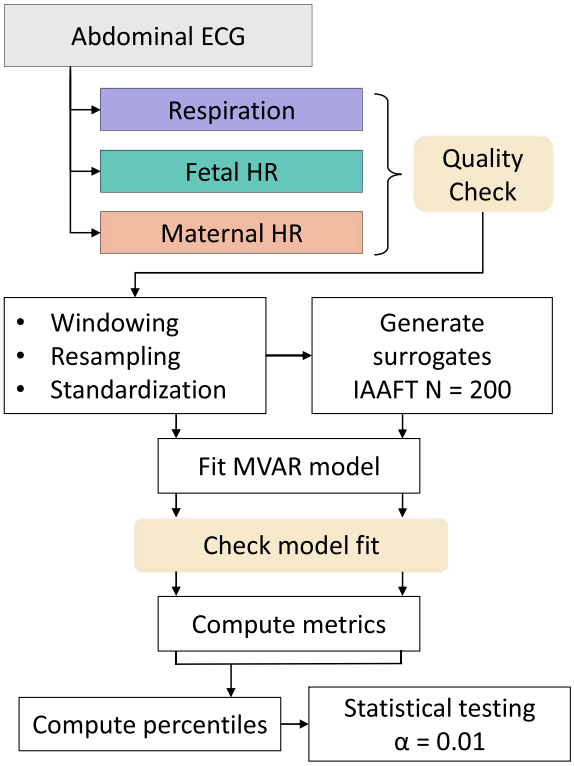

Fig. 1. Overview of the signal processing and analysis pipeline. Maternal abdominal ECG was used to extract respiration, fetal heart rate (FHR), and maternal heart rate (MHR), followed by quality check. Preprocessing included windowing, resampling, and standardization. Surrogate data were generated using Iterative Amplitude Adjusted Fuorier Transform (IAAFT) with N = 200. A multivariate autoregressive (MVAR) model was then fitted, with model fit evaluation. From the validated models, metrics were computed, percentiles estimated, and statistical testing performed ($\alpha = 0.01$).

metrics were computed. The same procedure was applied to all surrogate signals generated from that window (Section 2.3), and the values obtained from the real data were compared with those from the surrogates. Statistical significance was then assessed from the percentile rank of the real-signal metrics with respect to the surrogate distributions (Section 2.4). Fig. 1 presents a schematic summary of the methodology applied in this study.

2.1. Population and experimental setup

For the investigation envisioned in this study, we employed a dataset of abdominal electrophysiological recordings. The data were acquired according to a study protocol reviewed and approved by the medical ethical reviewing committee of the Máxima Medical Centre, Veldhoven, the Netherlands (NL48535.015.14). The dataset consists of 496 recordings from pregnant women carrying a singleton fetus with a gestational age (GA) between 18 and 24 weeks, corresponding to the mid-second trimester. ECGs were sampled at 500 Hz, and recordings lasted approximately 30 minutes. The signals were recorded using adhesive Ag/AgCl electrodes, which were positioned on the abdomen while the participants were in a semi-recumbent position. A total of eight electrodes were arranged in the configuration depicted in Fig. 2, generating six channels of bipolar recordings. The remaining two electrodes functioned as a common reference and ground. From the available dataset, we selected only the acquisitions belonging to healthy pregnancies ($N = 326$) and to fetuses with diagnosed CTA ($N = 17$). More details about the dataset can be found in [24].

2.2. Data preparation

To compute the coupling measures, the FHR, MHR, and respiratory signal were extracted from abdominal ECG signals. All analyses to extract the time series of interest were conducted on consecutive 1-minute windows of raw multichannel ECG data. An example of raw ECG and extracted signals is depicted in Fig. 3, where a clear synchronization between the MHR and the respiratory signal is visible. The extraction process was followed by a quality assessment to discard low-quality estimations that could compromise the accuracy of the coupling evaluation. Finally, the signals were segmented into 2-minute windows. The following sections detail the methods used.

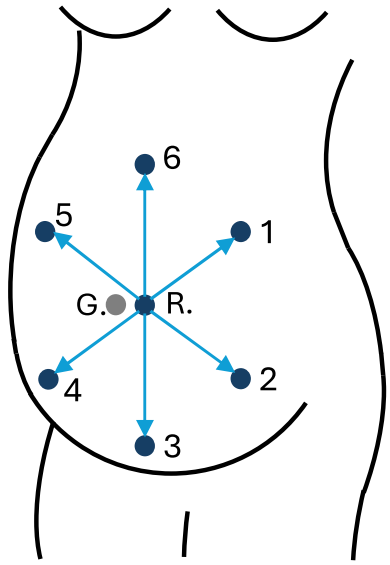

Fig. 2. Electrode Configuration. Active electrodes (blue circles) are placed in a bipolar configuration, with the reference electrode close to the navel. Ground (gray circle) is placed slightly above the reference. The bipolar channels, indicated by the arrows, are formed by electrodes 1–6 relative to the common reference.

2.2.1. Fetal and maternal heart rate

To estimate the FHR and MHR from the abdominal recordings, we employed a modified version of the algorithm presented in [25]. The algorithm relies on an iterative procedure based on periodic component analysis (πCA), a blind source separation technique based on signal periodicity, which isolates the component of interest, and singular value decomposition (SVD), which performs denoising. First, the mECG is isolated and used to estimate the MHR. Then, the mECG is subtracted from the raw signals, leaving only the residual fetal ECG (fECG) and noise. The procedure is then reapplied to these residual signals to isolate the fECG, which is employed to identify the fetal R peaks using the algorithm described by Varanini et al. [26]. The fetal R peaks were used to determine the FHR series. This method was chosen because, as reported in detail in [25], it has been shown to outperform other state-of-the-art approaches in deriving a robust FHR series from both in-silico and in-vivo abdominal ECG data.

The MHR and FHR were extracted from the abdominal ECG as sequences of beat-to-beat intervals, where each new value corresponds to the time elapsed since the previous R-peak. As a result, these series are irregularly sampled, and the maternal and fetal beats do not occur at the same instant. To enable synchronous analysis, both the MHR and FHR were resampled onto a common, uniformly spaced time axis. Specifically, we applied linear interpolation of MHR and FHR at equally spaced time points defined by a sampling interval of $1/Fs$, where Fs is set to 6 Hz. This frequency was selected since it corresponds to double the maximum expected FHR (i.e., 180 bpm), ensuring that there is no risk of aliasing and that all spectral components are correctly represented. Linear interpolation was preferred over other interpolation strategies, like cubic spline, to avoid introducing spurious spectral components.

2.2.2. ECG derived respiration

The respiration was derived from the multichannel mECG signals by analyzing the QRS amplitude modulation—a feature strongly influenced by respiration [27]. This effect arises from mechanical shifts in heart axis orientation and electrode position, and is therefore independent of the heart rate. To quantify it, the R peaks and corresponding S waves were detected from each channel to create the RS series. This series was then resampled to 6 Hz synchronously with the FHR and MHR, and used to identify the average respiratory frequency. Then, similarly to [28], the RS series was decomposed using multivariate variational mode decomposition (MVMD) [29] into its modes. The mode closer to the average respiratory frequency was retained as the respiration estimate. This mode was selected from the first channel, which had the highest average quality, defined as the percentage of spectral power within the physiological respiratory range (0.12–0.45 Hz) of the RS series. The superior quality of this channel is consistent with its proximity to the diaphragm, which increases its sensitivity to respiratory movements.

2.2.3. Windowing and quality check

The synchronous signals obtained in the previous steps were divided into 2-minute windows with an overlap of 50%. This length was selected to balance adequate reliability in model fitting with the requirement of stationarity. In adults, the optimal compromise is usually achieved with windows of 3–4 minutes [17,18]. To account for the faster dynamics of the FHR, shorter windows are used for its analysis [13]. Consequently, when investigating maternal–fetal interactions, window lengths of approximately 1–2 minutes are typically adopted [6,8].

To guarantee that only windows in which maternal respiration, MHR, and FHR are estimated correctly are included in the analysis, a quality check was introduced. The quality of the FHR signal samples is estimated based on the periodicity of the estimated fECG and physiological plausibility. In particular, windows are excluded if less than 25% of the

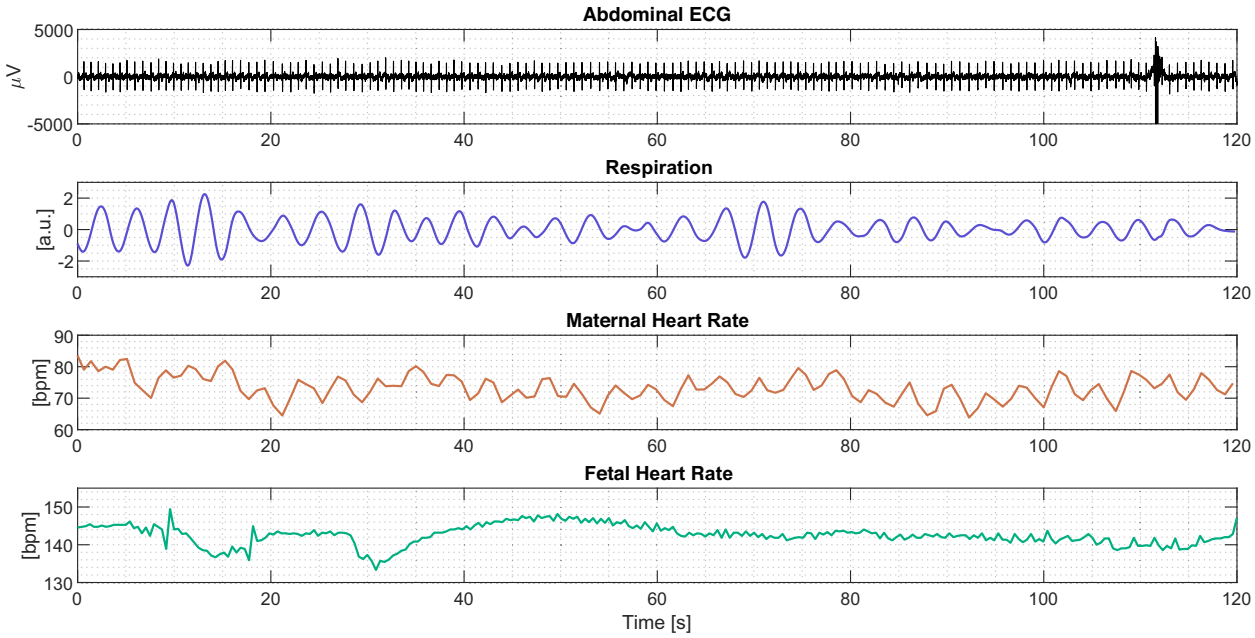

Fig. 3. Example of (single channel) raw signal and extracted time series.

fECG signal power is located within 0.4 Hz around the estimated mean FHR and its harmonics and if the median FHR is lower than 110 bpm or higher than 190 bpm, since values outside this range are not physiologically acceptable [30]. Moreover, single FHR samples are considered as "low quality" if the beat-to-beat variability exceeds a threshold of 50 ms because such a large change between adjacent beats is not physiological, indicating an incorrect estimation. Windows containing more than 5% low-quality samples were excluded from further analysis.

The quality of the respiratory signal is quantified by assessing the correlation in the frequency domain among the RS series estimated from each ECG channel and ensuring physiological plausibility. Specifically, the magnitude-squared coherence between the first channel (see Fig. 2) and the other five is computed within the respiratory band (0.12 – −0.45 Hz); only channels with a coherence greater than 0.6 are retained, and if fewer than three channels meet this criterion, the window is discarded. Subsequently, the Short-Time Fourier Transform with a 1-minute window and 80% overlap is applied to compute the time-varying respiratory frequency, which is then low-pass filtered using a 4-minute moving average. Windows in which the central frequency estimated via MVMD deviates by more than 0.1 Hz from the moving average are rejected. This step was implemented since, considering the experimental protocol, abrupt changes in the respiratory frequency are not expected and are likely errors in the mode selection. Errors in the detection of R peaks in the mECG were very rare, and did not warrant dedicated post-processing.

In the windows that meet the aforementioned quality checks, isolated low-quality FHR or MHR samples can still occur. For this reason, isolated outliers in the FHR and MHR were corrected using the Lipponen algorithm [31].

2.3. Coupling measures

In this work, coupling was estimated using linear metrics. The adoption of a linear approach was motivated by several factors. First, linear models require fewer parameters than their nonlinear counterparts, allowing reliable fitting with smaller datasets and reducing sensitivity to noise [32]. Second, they have a straightforward frequency-domain representation, which is particularly advantageous since CV signals are rich in harmonic content and well suited to spectral analysis [16]. Finally, linear models constitute the most established and widely validated framework for studying cardiovascular interactions [19], ensuring methodological robustness and comparability with previous research. Among the linear measures that have been proposed and applied for evaluating the short-term causal interactions among bio-signals [33], Directed Coherence (DC), PDC and gPDC have the advantages of: i) being able to identify (Granger) causal interactions and associated directionality; ii) providing meaningful results with relatively few samples; iii) showing positive findings from the application of the PDC on the FHR and MHR in previous literature [6]; iv) distinguishing between direct and indirect interactions via PDC and gPDC, which is a relevant property in the analysis of multivariate series.

In our analysis, we considered both bivariate (MHR – respiration, FHR – respiration, and MHR – FHR) and trivariate (MHR – FHR – respiration) modeling. For the bivariate case, the gPDC and the DC are identical. The gPDC is especially beneficial in scenarios with highly unbalanced predictive modeling errors (i.e., when time series are predicted by the model with significantly different errors), where it is more robust compared to the classical definition of PDC [34]. Moreover, it is insensitive to the variance of the input signals. This property is particularly useful in the current investigation due to the heterogeneous nature of the data in the analysis.

The mathematical background of DC, PDC, and gPDC is discussed in more detail in [17,35]. Their formulation is based on the concept of Granger-causality, which formalizes the idea that causes precede their effects in time. If the past of a time series contributes to predicting the future of another time series, then the first time series is said to Granger-cause the second one. This relationship can be estimated by fitting the data with a linear multivariate autoregressive (MVAR) model. When the model fits the data well, its coefficients capture the influence of the past values of each time series on the others. These coefficients serve as the foundation for computing DC, PDC, and gPDC.

The general formulation of an MVAR model is given by:

$$X[n] = \sum_{k=1}^{p} A[k]X[n-k] + W[n], \tag{1}$$

where $X[n]$ is the multivariate vector, $\mathbf{A}[k]$ contains the model coefficients and $W[n]$ represents white noise. In this model, each individual

time series within $X[n]$ is modeled as a linear combination of its own past values as well as the past values of all other time series in the vector, up to a maximum lag of p. The term $W[n]$ accounts for residual noise, and p denotes the model order.

For each 2-minute window, the MVAR model was fitted using least-squares optimization, with the optimal order determined via the Akaike Information Criterion. Before model fitting, all time series were linearly detrended and normalized to unit variance. Since the reliability of the measures depends on the validity of the model, the residuals were tested for whiteness using the Portmanteau test for autocorrelation and for independence via the Kendall test, setting the threshold alpha to 0.05, as in [17]. Only models with white and independent residuals were included for further analysis.

Then, the estimated matrix $\mathbf{A}[k]$ is utilized to compute the coupling measures after being transformed into the frequency domain, as described by the following equation, where T indicates the sampling period, and $H(f)$ is the transfer matrix of the filter $X(f) = H(f) \cdot W(f)$:

$$\mathbf{A}(f) = \sum_{k=1}^{p} \mathbf{A}(k) e^{-j2\pi f k T}, \qquad \mathbf{H}(f) = [I - \mathbf{A}(f)]^{-1} \tag{2}$$

2.3.1. Directed coherence

A straightforward formulation to quantify pairwise linear interactions is given by the *coherence* $\Gamma_{ij}(f)$:

$$S_{ij}(f) = \sum_{m=1}^{M} \sigma_m^2 H_{im}(f) H_{jm}^*(f), \qquad \Gamma_{ij}(f) = \frac{S_{ij}(f)}{\sqrt{S_{ii}(f) S_{jj}(f)}}, \tag{3}$$

where $S_{ij}(f)$ is the cross-spectral density matrix, σ_j represents the standard deviation of w_j and M is the number of modeled time series. Given its symmetry, $\Gamma_{ij}(f)$ does not indicate directionality, which motivates the introduction of the DC. The DC from series x_j to x_i can be derived by substituting $S_{ij}(f)$ into $\Gamma_{ij}(f)$ in Eq. (3), thus factorizing the coherence into its directional components, and is defined in the following:

$$DC_{ij}(f) = \frac{\sigma_j H_{ij}(f)}{\sqrt{\sum_{m=1}^{M} \sigma_m^2 \left[H_{im}(f)\right]^2}}. \tag{4}$$

Thus, $DC_{ij}(f)$ is a measure of the influence of x_j on x_i. Since $DC_{ij}(f)$ is normalized with respect to the receiving signal, it can be interpreted as a measure of the relative influence of x_j on x_i, normalized by all incoming influences on x_i, including its past. This complex function has an absolute value squared $|DC_{ij}(f)|^2$ which varies between 0 and 1 for each value of f due to the normalization factor in Eq. (4).

2.3.2. Partial directed coherence

One of the main limitations of the DC is that it does not distinguish between direct and indirect interactions. These can be overcome by the *partial coherence* $\Pi_{ij}(f)$, which measures the linear relationship between two signals after the influence of the other signals has been removed. Its formula is reported in the following:

$$P_{ij}(f) = \sum_{m=1}^{M} \overline{\mathbf{A}}_{mi}^*(f) \overline{\mathbf{A}}_{mj}(f), \qquad \Pi_{ij}(f) = \frac{P_{ij}(f)}{\sqrt{P_{ii}(f) P_{ij}(f)}}, \tag{5}$$

where $P_{ij}(f)$ is the inverse cross spectral density matrix and $\overline{A}(f) = [I - A(f)]$. To asses directionality, the $PDC(f)$ can be derived by factorizing the partial coherence after substituting $P_{ij}(f)$ into $\Pi_{ij}(f)$ in Eq. (3) and it is defined as:

$$PDC_{ij}(f) = \frac{\bar{A}_{ij}(f)}{\sqrt{\sum_{m=1}^{M} \left|\bar{A}_{mj}(f)\right|^2}}. \tag{6}$$

$PDC_{ij}(f)$ represents how strongly a signal source x_j interacts with the signal x_i, relative to all interactions of x_j with other signals. In this way, the PDC ranks the interaction strengths of a given signal source in comparison to its other connections. Notice that this normalization contrasts with the one used in $DC(f)$, which normalizes with respect to the receiving signal. Similarly to the DC, $|PDC_{ij}(f)|^2$ varies between 0 and 1 at each frequency.

The main advantage of the PDC compared to DC is its ability to distinguish between direct and indirect interactions, while DC provides a more interpretable and intuitive normalization [16].

2.3.3. Generalized partial directed coherence

The generalized PDC (gPDC) is a variation of the PDC that is unaffected by changes in signal variance while effectively distinguishing between direct and indirect interactions, and was proposed by Baccala et al.[34]. Its formula is given by:

$$gPDC_{ij}(f) = \frac{\frac{1}{\sigma_i} \bar{A}_{ij}(f)}{\sqrt{\sum_{m=1}^{M} \frac{1}{\sigma_m^2} \left|\bar{A}_{mj}(f)\right|^2}}. \tag{7}$$

Since we are interested only in the magnitude of the complex functions $DC_{ij}(f)$, $PDC_{ij}(f)$, and $gPDC_{ij}(f)$, and thanks to the normalization properties discussed, we analyze only $|DC_{ij}(f)|^2$, $|PDC_{ij}(f)|^2$, and $|gPDC_{ij}(f)|^2$.

The feature value selected to represent these functions is their integral between 0 and 1 Hz, as shown in yellow in Fig. 4, for the illustrative case of a bivariate analysis of FHR vs. respiration. This frequency band was selected since we do not expect any frequency content over 1 Hz for the MHR and respiration, making any apparent interactions among them and with the FHR meaningless. For simplicity, in the rest of the paper, we will refer to $\int_0^1 |DC_{ij}(f)|^2 \, df$ as DC, $\int_0^1 |PDC_{ij}(f)|^2 \, df$ as PDC, and $\int_0^1 |gPDC_{ij}(f)|^2 \, df$ as gPDC. In all figures and tables, the MHR is represented by the letter "M," the FHR by "F," and the respiratory signal by "R."

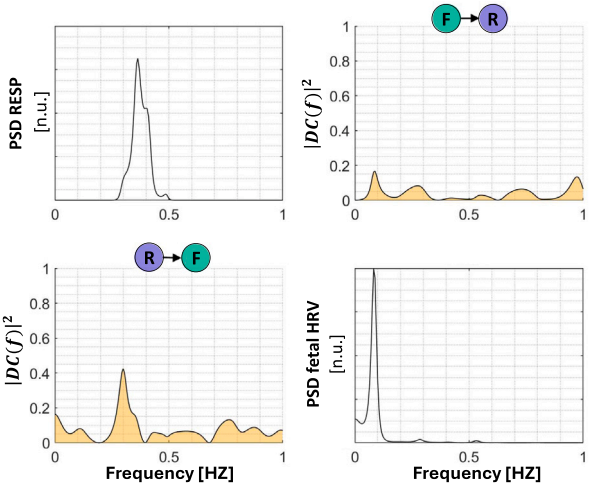

Fig. 4. The feature value DC is computed as the Area of $|DC_{ij}(f)|^2$ and is marked in yellow. The PSDs of maternal respiration and of the FHR are reported on the diagonal.

2.4. Statistical assessment

The magnitude of coupling measures depends on both the adopted normalization strategy and the frequency bandwidth over which the time series interact. Fig. 4 shows an applicative example in which the two signals interact only in a relatively narrow frequency band. Moreover, coupling measures can exhibit spurious small nonzero values even in the absence of genuine coupling between time series due to approximations in model estimation. As a result, absolute values alone are not inherently meaningful, but gain significance when interpreted comparatively. Consequently, significance testing using surrogate data is recommended to assess whether the value obtained is indicative of coupling [15]. In this study, we used comparison with surrogate data generated via the Iterated Amplitude Adjusted Fourier Transform with exact spectrum (IAAFT) [36]. This method has been extensively validated using simulated and real signals and applied to the analysis of cardiovascular signals [6,37]. Because IAAFT preserves the amplitude spectrum of the original signal in the surrogates, it reduces the risk of false positives by preventing spurious coupling detections caused by oscillations at similar frequencies but generated by unrelated mechanisms. At the same time, the randomized phase removes genuine temporal associations, thereby minimizing the risk of false negatives that could arise if the surrogates retained residual coupling. For each analyzed window, we generated 200 surrogate time series based on the real data. We then fitted an MVAR model to each surrogate and calculated the percentile rank of the real PDC and DC values relative to the distribution of the surrogates. In the absence of coupling, the expected distribution of the percentiles is uniform. If the distribution is left-skewed, the coupling in the real data is higher than in the surrogates. To test its significance, we employed a right-tailed Wilcoxon signed-rank test to determine whether the median is significantly greater than the expected value of 50%. Results are considered statistically significant if the p-value is less than or equal to 0.01. Effect sizes of significant connections were quantified with the rank-biserial correlation coefficient. A coefficient of 0 indicates no difference in coupling between the real and surrogate data, whereas a value of 1 indicates that the real data exhibited stronger coupling than all surrogates.

Analyses were performed on the healthy cohort ($N = 326$), which provides a sufficient sample size to robustly assess the significance and directionality of the interactions. As a proof of concept, the same analyses were also applied to the smaller pathological cohort ($N = 17$). Differences in the coupling measures between the two cohorts were evaluated using the Mann–Whitney U test. Comparisons were limited to interactions that reached statistical significance in the test against surrogate data.

3. Results

3.1. Coupling measures in healthy fetuses

3.1.1. Bivariate analysis

The results of bivariate modeling are summarized in Fig. 5, which illustrates the interactions identified. The absolute values of DC and PDC and the p-values obtained by the comparison with surrogate data are reported in Table 1. In bivariate analysis, gPDC values are not reported as they are identical to DC. Both DC and PDC detected a significant interaction from the respiration to the MHR ($p < 0.001$) and from the respiration to the FHR ($p < 0.001$). Additionally, DC identified a weak, but still significant ($p < 0.001$), interaction from the MHR to the respiration, which was not captured by PDC. Regarding the interaction between the MHR and the FHR, PDC detected a weak influence from the MHR to the FHR, whereas the other measure did not. None of the analyzed measures identify any interaction from the FHR to the MHR or from the FHR to the respiration.

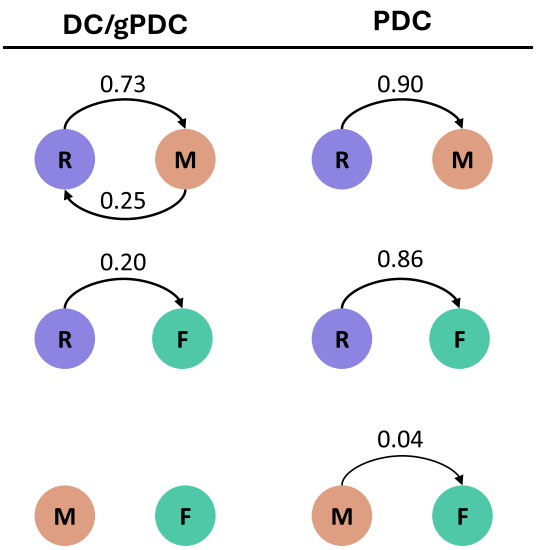

Fig. 5. Identified interactions in bivariate modeling for healthy fetuses. M indicates MHR, F indicate FHR and R indicates respiration. Arrows indicate significant interactions, numbers report the effect sizes.

3.1.2. Trivariate analysis

As shown in Fig. 6, results obtained modeling MHR, FHR and the respiratory signal together largely confirm results obtained in bivariate modeling: the maternal respiration acts as a common source of predictive influence for both the MHR and FHR, as identified by all analyzed measures. As can be deduced from Table 1, the relation from the respiration to the MHR is stronger than the relation from respiration to the FHR. Moreover, a weak interaction from MHR to respiration was identified by the DC and gPDC, but not by PDC. Interestingly, the interaction from MHR to FHR, which was captured by the PDC in bivariate modeling, disappears when the respiratory signal is included. This suggests that the interaction from the MHR to the FHR is at least partially mediated by maternal respiration.

To better illustrate the mechanism behind these coupling measures, an example showing the effect of respiration on partial cross-spectra, which are used to compute PDC and gPDC, is reported in Fig. 7. A direct interaction between the respiration and the MHR is evident, as indicated by the peak at around 0.37 Hz, which surpasses a coherence value of 0.6. Similarly, a weaker interaction (coherence ≈ 0.4) between the respiration and the FHR can be observed at around 0.48 Hz.

3.2. Comparison with CTA fetuses

As shown in Figs. 8 and 9, when considering only fetuses with CTA, neither DC nor gPDC detected any interaction between the fetus and the other time series, while PDC identified a weak interaction from the respiration to the FHR. No differences were identified in the interaction between the MHR and the respiration.

The absolute values of the analyzed metrics for fetuses with CTA, alongside the results of the comparison with healthy controls, are shown in Tables 2 and 3. Table 2 reports the bivariate analysis, while Table 3 shows the trivariate analysis. Only interactions that previously proved to be significant in at least one subgroup are considered. In the complete, trivariate model, CTA-affected fetuses present lower values for the measures of coupling according to DC and gPDC. In particular, gPDC and DC values from the MHR to the FHR showed a trend toward reduction that approached statistical significance. A more pronounced, and significant, reduction in coupling from respiration to FHR was observed using both gPDC and DC, but not PDC. This specific case is illustrated in Fig. 10.

Table 1
DC, PDC, and gPDC values (mean ±std) along with corresponding p-values for bivariate and trivariate analysis. M indicates MHR, F indicates FHR and R indicates respiration.

Int.	DC (mean ±std)	p-value	PDC (mean ±std)	p-value	gPDC (mean ±std)	p-value
Bivariate Analysis						
M→F	0.04 ±0.03	0.138	0.10 ±0.12	**0.001**	–	–
F→M	0.03 ±0.03	0.401	0.03 ±0.05	0.865	–	–
R→M	0.08 ±0.04	<**0.001**	0.52 ±0.22	<**0.001**	–	–
M→R	0.05 ±0.03	<**0.001**	0.00 ±0.01	1	–	–
R→F	0.05 ±0.04	<**0.001**	0.54 ±0.25	<**0.001**	–	–
F→R	0.04 ±0.04	0.074	0.00 ±0.01	1	–	–
Trivariate Analysis						
M→F	0.04 ± 0.03	0.206	0.11 ± 0.13	0.034	0.04 ± 0.03	0.336
F→M	0.04 ± 0.03	0.829	0.05 ± 0.07	0.713	0.04 ± 0.03	0.855
R→M	0.07 ± 0.05	<**0.001**	0.35 ± 0.22	<**0.001**	0.07 ± 0.04	<**0.001**
M→R	0.05 ± 0.03	<**0.001**	0.00 ± 0.01	1	0.05 ± 0.03	<**0.001**
R→F	0.04 ± 0.04	<**0.001**	0.35 ± 0.24	<**0.001**	0.04 ± 0.04	**0.006**
F→R	0.04 ± 0.03	0.102	0.00 ± 0.00	1	0.04 ± 0.03	0.072

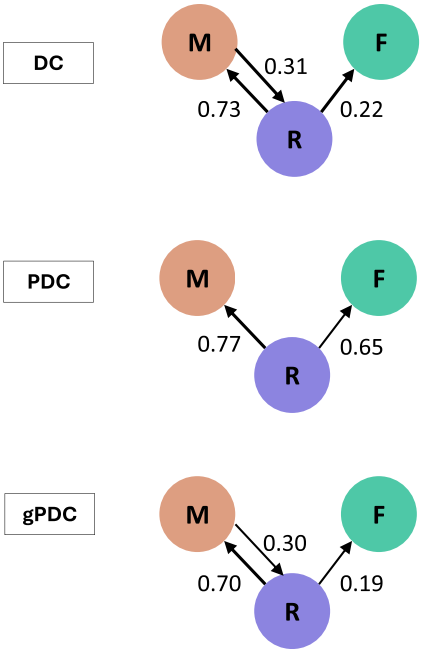

Fig. 6. Identified interactions in trivariate modeling for healthy fetuses. M indicates MHR, F indicate FHR and R indicates respiration. Arrows indicate significant interactions, numbers report the effect sizes.

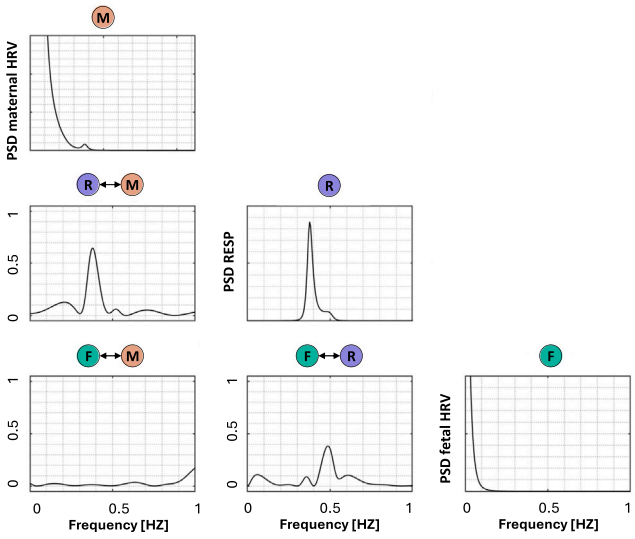

Fig. 7. Panels on the diagonal depict the estimated PSDs. Values are in arbitrary units following signal normalization. The other panels depict the partial cross-spectra. M indicates MHR, F indicates FHR, and R indicates respiration.

4. Discussion

In this study, we investigated MFCC by quantifying the interactions among MHR, FHR, and maternal respiration using linear metrics, with the aim of identifying significant interactions and determining their directionality. The results reported in Figs. 4 and 5, and Table 1 suggest that in healthy fetuses between 18 and 24 weeks of gestational age, short-term Granger causal interactions between MHR and FHR are mainly modulated by maternal respiration, which acts as a common source of predictive influence for both signals. As shown in Table 1, all metrics consistently reveal a significant influence of respiration on both FHR and MHR ($p < 0.001$) compared to surrogate data. Furthermore, the small relationship observed between the MHR and the FHR when considering these two time series alone is attenuated when the respiratory signal is included in the analysis. These findings support the hypothesis that maternal respiration plays a key role in modulating both maternal and fetal heart rate dynamics.

Some of these findings are consistent with the existing literature, particularly the well-known causal influence of respiration on the MHR, which is mediated by established autonomic mechanisms [17]. However, the observed influence of maternal respiration on FHR represents a novel contribution, as, to the best of our knowledge, this relationship has not been directly investigated in the human fetus. Methodologically, it is crucial to stress that the metrics analyzed in this study quantify Granger causality, which reflects predictive influence and temporal precedence. While these results support the existence of a connection, they cannot directly prove that this connection is mechanistic, as this conclusion would require other invasive experiments. Consequently, at this stage of the research, we can only provide speculative hypotheses about the nature of the interaction.

One of these hypotheses is that the modulatory effect of the maternal respiration may be related to the variations in maternal arterial blood pressure, which oscillates around its mean synchronously with the

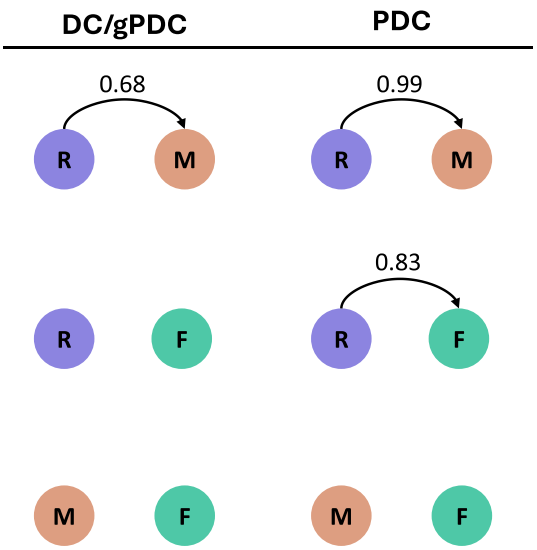

Fig. 8. Identified interactions in bivariate modeling for CTA subjects. Arrows indicate significant interactions, numbers report the effect sizes.

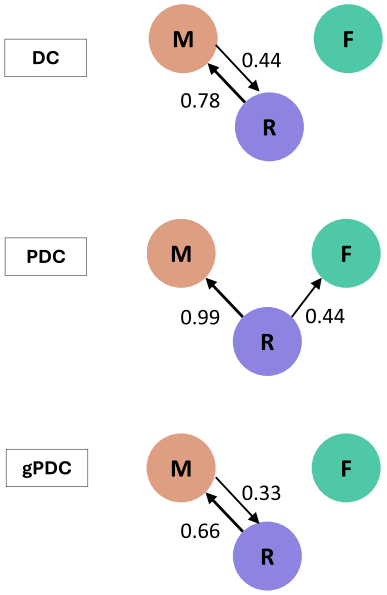

Fig. 9. Identified interactions in trivariate modeling for CTA subjects. Arrows indicate significant interactions, numbers report the effect sizes.

Table 2
DC, PDC, and gPDC values (mean ±std) and corresponding p-values for CTA affected fetuses computed with bivariate modeling. ↓ indicates lower values for CTA compared to controls.

	Interaction	DC/gPDC	PDC
Absolute values	M→F	0.03 ±0.02	0.09 ±0.09
	R→M	0.08 ±0.04	0.54 ±0.19
	M→R	0.04 ±0.02	0.00 ±0.00
	R→F	0.03 ±0.03	0.33 ±0.19
p-values comparison with healthy fetuses	M→F	0.077	0.856
	R→M	0.910	0.730
	M→R	0.253	0.779
	R→F	0.189	0.729

respiration [38]. It is reasonable to hypothesize that these fluctuations may affect placental oxygen transfer from the placenta to the fetus.

Table 3
DC, PDC, and gPDC values (mean ±std) and corresponding p-values for CTA affected fetuses computed with trivariate modeling. ↓ indicates lower values for CTA compared to Controls.

Interaction	DC	PDC	gPDC
Absolute values			
M→F	0.03 ±0.03	0.09 ±0.12	0.07 ±0.03
R→M	0.07 ±0.05	0.40 ±0.18	0.07 ±0.05
M→R	0.04 ±0.02	0.00 ±0.00	0.04 ±0.02
R→F	0.03 ±0.03	0.33 ±0.19	0.03 ±0.03
p-values – comparison with healthy fetuses			
M→F	0.052 ↓	0.516	0.041 ↓
R→M	0.533	0.159	0.574
M→R	0.742	0.399	0.774
R→F	**0.008** ↓	0.914	**0.005** ↓

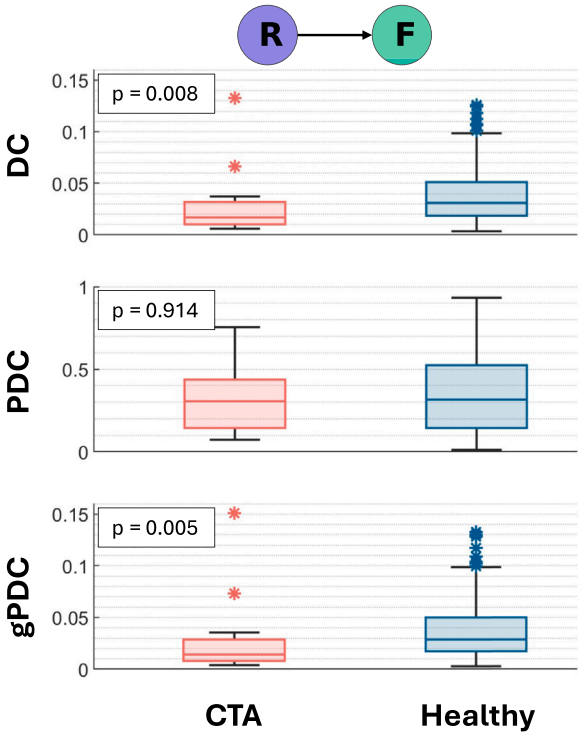

Fig. 10. Comparison of coupling measured from respiration to FHR in CTA-affected and Healthy fetuses.

Given that FHR is known to adapt in response to changes in oxygen availability [39,40], this mechanism could underlie the observed respiratory-related modulation of FHR. Another hypothesis is that this modulatory effect may be mediated by the fetal autonomic nervous system. In fact, mild external compression has been associated with increased parasympathetic activity in infants [41], suggesting that the fetal autonomic response to respiratory - induced compression may also mediate the interaction between maternal respiration and FHR.

Although the results obtained with DC, PDC, and gPDC are largely consistent, there are some differences that warrant closer examination. In particular, PDC tends to polarize the results relative to DC and gPDC. Specifically, it does not detect bidirectional interactions, such as those observed between MHR and respiration by both DC and gPDC, and yields values that are often either near 0 or near 1, corresponding to the lowest and highest possible values. This difference can probably be attributed to the different normalization strategies adopted. Indeed, the magnitude value of PDC reflects information flow through the inverse spectral matrix, which cannot be straightforwardly interpreted in terms of power

spectral density, and the normalization is performed with respect to the source signal (conversely to DC, which normalizes with respect to the receiving signal). As discussed in [16], these elements make PDC a useful metric to identify causal directed interactions, but also make it a poor indicator of the coupling strength. In general, it is important to emphasize that, because of how the presented metrics are computed, particularly the normalization and integration steps, the absolute values alone provide limited insight into the actual coupling strength also for the DC and the gPDC. Indeed, by construction, a value of 1 would imply that one signal fully explains another across all frequencies, which is physiologically unrealistic given the complex dynamics of the analyzed signals. In practice, coupling may appear only in narrow bands (e.g., respiration), so integrated values over the full spectrum are often very small, even for well-documented phenomena such as RSA. For this reason, absolute magnitudes provide limited insight, and are more meaningful when interpreted comparatively. For example, the values obtained using DC and gPDC for the interaction from respiration to FHR (0.04 ± 0.04 for both metrics in the trivariate analysis) are statistically significant, despite their small magnitude, as indicated by the corresponding p-values (< 0.001 and 0.006, respectively). These values are notably lower than those observed for the interaction from respiration to MHR (0.07 ± 0.05), which is also significant ($p < 0.001$), and reflect the well-known physiological phenomenon known as respiratory sinus arrhythmia [12]. This suggests that the influence of respiration on FHR is weaker than its effect on MHR, which is consistent with the expected physiological behavior. The limited physiological interpretability of the absolute values of the coupling metrics discussed presents a challenge for clinical application. To address this, alternative normalization strategies and different feature representations of the PDC, DC, and gPDC functions - such as using the maximum value instead of the integral - will be explored to facilitate their use in clinical context.

Our results may serve as a foundation for future clinical investigations aimed at assessing the relationship between impaired coupling and cardiovascular maternal or fetal pathology. In this context, the results reported in Table 3 and Figs. 9 and 10 provide a first preliminary evidence that CTA-affected fetuses present a reduced response to maternal respiration. The Granger causal interaction from the respiration to the FHR was indeed not significant for DC and gPDC in the pathological population, where it also assumed significantly lower absolute values compared to healthy fetuses, and was associated with a higher p-value for PDC.

The physiological mechanisms underlying the observed reduction in the modulation of the FHR by maternal respiration in the CTA cohort remain uncertain. A possible explanation involves structural circulatory alterations, such as changes in cerebral blood flow, which have been proposed to impair brainstem regulation of autonomic activity [42]. Such alterations could, in turn, attenuate the respiratory influence on FHR.

Overall, these results are encouraging for advancing our understanding of pregnancy physiology and point toward potential clinical relevance. Nevertheless, they remain preliminary and more research is needed to further explore the clinical implications of these findings. To this end, future studies should focus on larger, multi-center cohorts. Regarding the pathological population, the CTA population served here as a preliminary proof-of-concept. In future studies, a larger sample size is required to stratify the analysis across CTA subtypes and include the evaluation of other pathologies. In particular, we believe it is highly relevant to investigate whether the role of maternal respiration in MFCC is altered in pathologies of pregnancy characterized by impaired placental transmission, such as fetal growth restriction.

Another aspect that remains to be clarified is how the relationship between maternal respiration and the FHR evolves during gestation. The analysis conducted in this study focuses on early pregnancy (18–24 weeks of gestation), a crucial phase during which the early detection of pathological conditions may enable timely and better treatment of the pathologies and, ultimately, improve pregnancy outcomes. However, the fetal autonomic nervous system develops progressively during pregnancy, and other physiological mechanisms that develop later in pregnancy, such as fetal behavioral states, may affect MFCC. This highlights the importance of longitudinal assessment to understand the evolution of coupling dynamics. To address this, our future developments will focus on the longitudinal assessment of MFCC with the inclusion of maternal respiration across different gestational ages and pathologies. Additionally, paced-respiration protocols will be used to more directly validate the identified relationships, and other physiological factors, such as arterial blood pressure and placental hemodynamics, will be included in the modeling framework.

5. Conclusion

In this study, we analyzed the short-term Granger causal interactions between the maternal and fetal heart rates and the role of maternal respiration in their modulation. Results suggest that, at the early GAs investigated, respiration can act as a source of influence that modulates both the MHR and FHR. This interaction, which has not been previously reported, may be responsible for all or part of the short-term coupling between the MHR and FHR, which do not appear to influence each other directly if maternal respiration is taken into account. This advances our understanding of MFCC and suggests that maternal respiration should be considered when modeling MFCC to avoid identifying spurious interactions. Moreover, preliminary results suggest that this phenomenon is impeded in the presence of conotruncal anomalies, suggesting that it may be helpful in the early detection of pregnancy complications.

CRediT authorship contribution statement

G. Steyde: Writing – review & editing, Writing – original draft, Visualization, Validation, Software, Methodology, Investigation, Formal analysis, Data curation, Conceptualization. **A. Galli:** Writing – review & editing, Validation, Supervision, Methodology, Investigation, Funding acquisition, Formal analysis, Conceptualization. **E. Peri:** Writing – review & editing, Validation, Supervision, Methodology, Resources, Project administration, Conceptualization. **M.B. Van der Hout-van der Jagt:** Writing – review & editing, Resources, Formal analysis. **J.O.E.H. Van Laar:** Writing – review & editing, Supervision, Resources, Data curation. **M.G. Signorini:** Writing – review & editing, Supervision, Resources, Project administration, Investigation, Funding acquisition. **M. Mischi:** Writing – review & editing, Supervision, Resources, Project administration, Funding acquisition, Conceptualization.

Ethics Statement

This study was reviewed and approved by the Ethics Committee of the Máxima Medical Centre, Veldhoven, the Netherlands, for research involving human participants, with the approval number NL48535.015.14. No animal experiments were involved in this study. All human experiments were conducted with the approval of the aforementioned ethics committee. Written informed consent was obtained from the participants. All experiments were conducted in accordance with the Helsinki Declaration.

Declaration of competing interests

The authors declare the following financial interests/personal relationships that may be considered potential competing interests:

Alessandra Galli reports financial support was provided by European Commission. Giulio Steyde reports financial support was provided by European Commission. If there are other authors, they declare that they have no known competing financial interests or personal relationships that could have appeared to influence the work reported in this paper.

Acknowledgment

G. Steyde is supported by: MUSA – Multilayered Urban Sustainability Action –project, funded by the European Union – NextGenerationEU, under the National Recovery and Resilience Plan (NRRP) project

no. ECS 00000037. A. Galli is supported by the European Union's Horizon Europe research and innovation programme under the Marie Sklodowska-Curie Postdoctoral Fellowship, project no. 101063008.

Code and data availability

The clinical data used in this study were obtained from a third party and are available from the original source [24] subject to their data access procedures. The code used in this study is proprietary and not publicly available.

References

[1] M. Sanghavi, J.D. Rutherford, Cardiovascular physiology of pregnancy, Circulation 130 (12) (2014) 1003–1008, https://doi.org/10.1161/CIRCULATIONAHA.114.009029

[2] G. Pardi, A.M. Marconi, I. Cetin, Placental-fetal interrelationship in IUGR fetuses—a review, Placenta 23 (2002) S136–S141, https://doi.org/10.1053/plac.2002.0802

[3] N. Itani, K.L. Skeffington, C. Beck, Y. Niu, G. Katzilieris-Petras, N. Smith, D.A. Giussani, Protective effects of Pravastatin on the embryonic cardiovascular system during hypoxic development, The FASEB Journal 34 (12) (2020) 16504–16515, https://doi.org/10.1096/fj.202001743r

[4] S. Lunshof, K. Boer, H. Wolf, G. van Hoffen, N. Bayram, M. Mirmiran, Fetal and maternal diurnal rhythms during the third trimester of normal pregnancy: outcomes of computerized analysis of continuous twenty-four—hour fetal heart rate recordings, Am. J. Obstet. Gynecol. 178 (2) (1998) 247–254, https://doi.org/10.1016/S0002-9378(98)80008-2

[5] T.J. Nichting, M. Bester, R. Joshi, M. Mischi, M. van der Ven, D.A.A. van der Woude, S.G. Oei, J.O.E.H. van Laar, R. Vullings, Evidence and clinical relevance of maternal-fetal cardiac coupling: a scoping review, PLOS ONE 18 (7) (2023) e0287245, https://doi.org/10.1371/journal.pone.0287245

[6] A.H. Khandoker, F. Marzbanrad, A. Voss, S. Schulz, Y. Kimura, M. Endo, M. Palaniswami, Analysis of maternal–fetal heart rate coupling directions with partial directed coherence, Biomed. Signal Process. Control 30 (2016) 25–30, https://doi.org/10.1016/j.bspc.2016.06.010

[7] A.H. Khandoker, S. Schulz, H.M. Al-Angari, A. Voss, Y. Kimura, Alterations in maternal-fetal heart rate coupling strength and directions in abnormal fetuses, Front. Physiol. 10 (APR) (Apr 2019), https://doi.org/10.3389/fphys.2019.00482

[8] F. Marzbanrad, Y. Kimura, M. Palaniswami, A.H. Khandoker, Quantifying the interactions between maternal and fetal heart rates by transfer entropy, PLOS ONE 10 (12) (2015) 1–13, https://doi.org/10.1371/journal.pone.0145672

[9] S.M. Lobmaier, A. Müller, C. Zelgert, C. Shen, P.C. Su, G. Schmidt, B. Haller, G. Berg, B. Fabre, J. Weyrich, H.T. Wu, M.G. Frasch, M.C. Antonelli, Fetal heart rate variability responsiveness to maternal stress, non-invasively detected from maternal transabdominal ECG, Arch. Gynecol. Obstet. 301 (2019) 405–414, https://doi.org/10.1007/s00404-019-05390-8

[10] J.A. DiPietro, R.S. Raghunathan, H.-T. Wu, J. Bai, H. Watson, F.P. Sgambati, J.L. Henderson, G.W. Pien, Fetal heart rate during maternal sleep, Dev. Psychobiol. 63 (5) (2021) 945–959, https://doi.org/10.1002/dev.22118

[11] E. Ferrazzi, G. Pardi, P.L. Setti, M. Rodolfi, S. Civardi, S. Cerutti, Power spectral analysis of the heart rate of the human fetus at 26 and 36 weeks of gestation, Clin. Phys. Physiol. Meas. 10 (1989) 57–60, https://doi.org/10.1088/0143-0815/10/4b/009

[12] F. Yasuma, J.-I. Hayano, Respiratory sinus arrhythmia, Chest 125 (2) (2004) 683–690, https://doi.org/10.1378/chest.125.2.683

[13] S. Cerutti, S. Civardi, A. Bianchi, M.G. Signorini, E. Ferrazzi, G. Pardi, Spectral analysis of antepartum heart rate variability, Clin. Phys. Physiol. Meas. 10 (1989) 27–31, https://doi.org/10.1088/0143-0815/10/4b/004

[14] P. Van Leeuwen, D. Geue, M. Thiel, D. Cysarz, S. Lange, M.C. Romano, N. Wessel, J. Kurths, D.H. Grönemeyer, Influence of paced maternal breathing on fetal-maternal heart rate coordination, Proc. Natl. Acad. Sci. 106 (33) (2009) 13661–13666, https://doi.org/10.1073/pnas.0901049106

[15] L. Faes, A. Porta, G. Nollo, Testing frequency-domain causality in multivariate time series, IEEE Trans. Biomed. Eng. 57 (8) (2010) 1897–1906, https://doi.org/10.1109/TBME.2010.2042715

[16] L. Faes, G. Nollo, Multivariate frequency domain analysis of causal interactions in physiological time series, In A.N. Laskovski (Ed.), Biomedical Engineering, Trends in Electronics, Communications and Software, InTech, 2011, https://doi.org/10.5772/13065

[17] L. Faes, S. Erla, A. Porta, G. Nollo, A framework for assessing frequency domain causality in physiological time series with instantaneous effects, Philos. Trans. R. Soc. A: Math. Phys. Eng. Sci. 371 (1997) (Aug 2013), https://doi.org/10.1098/rsta.2011.0618

[18] A. Porta, T. Bassani, V. Bari, G.D. Pinna, R. Maestri, S. Guzzetti, Accounting for respiration is necessary to reliably infer granger causality from cardiovascular variability series, IEEE Trans. Biomed. Eng. 59 (3) (2012) 832–841, https://doi.org/10.1109/TBME.2011.2180379

[19] V. Pichot, C. Corbier, F. Chouchou, The contribution of Granger causality analysis to our understanding of cardiovascular homeostasis: from cardiovascular and respiratory interactions to central autonomic network control, Front. Netw. Physiol. 4 (2024), https://doi.org/10.3389/fnetp.2024.1315316

[20] T.R. Johnson, Conotruncal cardiac defects: a clinical imaging perspective, Pediatr. Cardiol. 31 (3) (2010) 430–437, https://doi.org/10.1007/s00246-010-9668-y

[21] E. Tegnander, S.H. Eik-Nes, The examiner's ultrasound experience has a significant impact on the detection rate of congenital heart defects at the second-trimester fetal examination, Ultrasound Obstet. Gynecol. 28 (1) (2006) 8–14, https://doi.org/10.1002/uog.2804

[22] C.L. van Velzen, J.C.F. Ket, P.M. van de Ven, N.A. Blom, M.C. Haak, Systematic review and meta-analysis of the performance of second-trimester screening for prenatal detection of congenital heart defects, Int. J. Gynecol. Obstet. 140 (2) (2017) 137–145, https://doi.org/10.1002/ijgo.12373

[23] K.L. Brown, Delayed diagnosis of congenital heart disease worsens preoperative condition and outcome of surgery in neonates, Heart 92 (9) (2006) 1298–1302, https://doi.org/10.1136/hrt.2005.078097

[24] C. Lempersz, J.O. van Laar, S.-A.B. Clur, K.M. Verdurmen, G.J. Warmerdam, J. van der Post, N.A. Blom, T. Delhaas, S.G. Oei, R. Vullings, The standardized 12-lead fetal electrocardiogram of the healthy fetus in mid-pregnancy: a cross-sectional study, PLOS ONE 15 (4) (2020) 1–12, https://doi.org/10.1371/journal.pone.0232606

[25] A. Galli, E. Peri, P. Hamelmann, M. Mischi, Improved mECG removal and fECG extraction by integrated periodic components analysis and singular value decomposition, in: 2024 IEEE International Symposium on Medical Measurements and Applications (MeMeA), IEEE, 2024, pp. 1–6, https://doi.org/10.1109/memea60663.2024.10596833

[26] M. Varanini, G. Tartarisco, L. Billeci, A. Macerata, G. Pioggia, R. Balocchi, An efficient unsupervised fetal QRS complex detection from abdominal maternal ECG, Physiol. Meas. 35 (8) (2014) 1607–1619, https://doi.org/10.1088/0967-3334/35/8/1607

[27] P.H. Charlton, T. Bonnici, L. Tarassenko, D.A. Clifton, R. Beale, P.J. Watkinson, An assessment of algorithms to estimate respiratory rate from the electrocardiogram and photoplethysmogram, Physiol. Meas. 37 (4) (2016) 610–626, https://doi.org/10.1088/0967-3334/37/4/610

[28] D. Labate, F. Foresta la, G. Occhiuto, F.C. Morabito, A. Lay-Ekuakille, P. Vergallo, Empirical mode decomposition VS. Wavelet decomposition for the extraction of respiratory signal from single-channel ECG: a comparison, IEEE Sens. J. 13 (7) (2013) 2666–2674, https://doi.org/10.1109/JSEN.2013.2257742

[29] N. ur Rehman, H. Aftab, Multivariate variational mode decomposition, IEEE Trans. Signal Process. 67 (23) (2019) 6039–6052, https://doi.org/10.1109/tsp.2019.2951223

[30] D. Ayres-de-Campos, C.Y. Spong, E. Chandraharan, FIGO consensus guidelines on intrapartum fetal monitoring: cardiotocography, Int. J. Gynecol. Obstet. 131 (1) (2015) 13–24, https://doi.org/10.1016/j.ijgo.2015.06.020

[31] J.A. Lipponen, M.P. Tarvainen, A robust algorithm for heart rate variability time series artefact correction using novel beat classification, J. Med. Eng. Technol. 43 (3) (2019) 173–181, https://doi.org/10.1080/03091902.2019.1640306

[32] L. Barnett, A.B. Barrett, A.K. Seth, Granger causality and transfer entropy are equivalent for Gaussian variables, Phys. Rev. Lett. 103 (23) (Dec 2009), https://doi.org/10.1103/physrevlett.103.238701

[33] S. Schulz, F.-C. Adochiei, I.-R. Edu, R. Schroeder, H. Costin, K.-J. Bär, A. Voss, Cardiovascular and cardiorespiratory coupling analyses: a review, Philos. Trans. R. Soc. A: Math. Phys. Eng. Sci. 371 (Aug 2013), https://doi.org/10.1098/rsta.2012.0191

[34] L.A. Baccala, K. Sameshima, D. Takahashi, Generalized partial directed coherence, in: 15th International Conference on Digital Signal Processing, 2007, pp. 163–166. doi:https://doi.org/10.1109/ICDSP.2007.4288544.

[35] L.A. Baccalá, K. Sameshima, Partial directed coherence: twenty years on some history and an appraisal, Biol. Cybern. 115 (3) (2021) 195–204, https://doi.org/10.1007/s00422-021-00880-y

[36] G. Lancaster, D. Iatsenko, A. Pidde, V. Ticcinelli, A. Stefanovska, Surrogate data for hypothesis testing of physical systems, Phys. Rep. 748 (2018) 1–60, https://doi.org/10.1016/j.physrep.2018.06.001

[37] L. Faes, G.D. Pinna, A. Porta, R. Maestri, G. Nollo, Surrogate data analysis for assessing the significance of the coherence function, IEEE Trans. Biomed. Eng. 51 (7) (2004) 1156–1166, https://doi.org/10.1109/TBME.2004.827271

[38] J.-L. Elghozi, D. Laude, A. Girard, Effects of respiration on blood pressure and heart rate variability in humans, Clin. Exp. Pharmacol. Physiol. 18 (11) (1991) 735–742, https://doi.org/10.1111/j.1440-1681.1991.tb01391.x

[39] Z.-Y. Yu, E.R. Lumbers, K.J. Gibson, A.D. Stevens, Effects of hypoxaemia on foetal heart rate, variability and cardiac rhythm, Clin. Exp. Pharmacol. Physiol. 25 (7–8) (1998) 577–584, https://doi.org/10.1111/j.1440-1681.1998.tb02255.x

[40] C.C. Heuser, Physiology of fetal heart rate monitoring, Clin. Obstet. Gynecol. 63 (3) (2020) 607–615, https://doi.org/10.1097/GRF.0000000000000553

[41] P. Franco, S. Scaillet, J. Groswasser, A. Kahn, Increased cardiac autonomic responses to auditory challenges in swaddled infants, Sleep 27 (8) (2004) 1527–1532, https://doi.org/10.1093/sleep/27.8.1527

[42] S. Siddiqui, A. Wilpers, M. Myers, J.D. Nugent, W.P. Fifer, I.A. Williams, Autonomic regulation in fetuses with congenital heart disease, Early Hum. Dev. 91 (3) (2015) 195–198, https://doi.org/10.1016/j.earlhumdev.2014.12.016